# Implementation and Performance of the High-Level Trigger electron and photon selection for the ATLAS experiment at the LHC

M. Diaz Gomez on behalf of the ATLAS HLT group*[1]

*Abstract*

The ATLAS experiment at the Large Hadron Collider (LHC) will face the challenge of efficiently selecting interesting candidate events in pp collisions at 14 TeV center-of-mass energy, whilst rejecting the enormous number of background events, stemming from an interaction rate of about $10^9$ Hz. The Level-1 trigger will reduce the incoming rate to around O(75 kHz). Subsequently, the High-Level Trigger (HLT), which comprises the second level trigger and the event filter, will reduce this rate further by a factor of O($10^3$). The HLT selection is software based and will be implemented on commercial CPUs using a common framework, which uses the standard ATLAS object-oriented software architecture. An overview of the current implementation of the selection for electrons and photons in the trigger is given. The performance of this implementation has been evaluated using Monte Carlo simulations in terms of the efficiency for the signal channels, the rate expected for the selection, the data preparation times, and the algorithm execution times. Besides the efficiency and rate estimates, a real physics example will be discussed, showing that the triggers are well adapted for the physics program envisaged at the LHC.

*S. Armstrong[a], A. dos Anjos[r], J.T.M. Baines[c], C.P. Bee[d], M. Biglietti[e], J.A. Bogaerts[f], V. Boisvert[f], M. Bosman[g], B. Caron[h], P. Casado[g], G. Cataldi[i], D. Cavalli[j], M. Cervetto[k], G. Comune[l], P. Conde Muíño[f], A. De Santo[m], M. Diaz Gomez[n], M. Dosil[g], N. Ellis[f], D. Emeliyanov[c], B. Epp[o], S. Falciano[p], A. Farilla[q], S. George[m], V. Ghete[o], S. González[r],M. Grothe[f], S. Kabana[l], A. Khomich[s], G. Kilvington[m], N. Konstantinidis[s], A. Kootz[t], A. Lowe[m], L. Luminari[p], T. Maeno[f],J. Masik[v], A. Di Mattia[p], C. Meessen[d], A.G. Mello[b], G. Merino[g], R. Moore[h], P. Morettini[k], A. Negri[w], N. Nikitin[x],A. Nisati[p], C. Padilla[f], N. Panikashvili[y], F. Parodi[k], V. Perez Reale[l], J.L. Pinfold[h], P. Pinto[f], Z. Qian[d], S. Resconi[j], S. Rosati[f], C. Sanchez[g], C. Santamarina[f], D.A. Scannicchio[w], C. Schiavi[k], E. Segura[g], J.M. de Seixas[b], S. Sivoklokov[x], Soluk[h], E. Stefanidis[t], R. S. Sushkov[g], M. Sutton[t], S. Tapprogge[z], E. Thomas[l], F. Touchard[d], B. Venda Pinto[aa], V. Vercesi[w], P. Werner[f], S. Wheeler[h bb], F.J. Wickens[c], W. Wiedenmann[r], M. Wielers[c], H. Zobernig[r] [a]Brookhaven National Laboratory (BNL), Upton, New York, USA. [b]Universidade Federal do Rio de Janeiro, COPPE/EE, Rio de Janeiro, Brazil. [c]Rutherford Appleton Laboratory, Chilton, Didcot, UK. [d] Centre de Physique des Particules de Marseille, IN2P3-CNRS-Université d´ Aix-Marseille 2, France [e]University of Michigan, Ann Arbor, Michigan, USA. [f]CERN, Geneva, Switzerland. [g] Institut de Física d´ Altes Energies (IFAE), Universidad Autónoma de Barcelona, Barcelona, Spain. [h]University of Alberta, Edmonton, Canada. [i]Dipartimento di Fisica dell´ Università di Lecce e I.N.F.N., Lecce, Italy. [j]Dipartimento di Fisica dell´ Università di Milano e I.N.F.N., Milan, Italy. [k]Dipartimento di Fisica dell´ Università di Genova e I.N.F.N., Genova, Italy. [l]Laboratory for High Energy Physics, University of Bern, Switzerland. [m]Department of Physics, Royal Holloway, University of London, Egham, UK. [n]Section de Physique, Université de Genève, Switzerland. [o]Institut für Experimentalphysik der Leopald-Franzens Universität, Innsbruck, Austria. [p]Dipartimento di Fisica dell´ Università di Roma ´ La Sapienza´ e I.N.F.N., Rome, Italy. [q]Dipartimento di Fisica dell´ Università di Roma ´ Roma Tre´ e I.N.F.N., Rome, Italy. [r]Department of Physics, University of Wisconsin, Madison, Wisconsin, USA. [s]Lehrstuhl für Informatik V, Universität Mannheim, Mannheim, Germany. [t]Department of Physics and Astronomy, University College London, London, UK. [u]Fachbereich Physik, Bergische Universitat Wuppertal, Germany. [v]Institute of Physics, Academy of Sciences of the Czech Republic, Prague, Czech Republic. [w]Dipartimento di Fisica Nucleare e Teorica dell´ Università di Pavia e INFN, Pavia, Italy. [x]Institute of Nuclear Physics, Moscow State University, Moscow, Russia. [y]Department of Physics, Technion, Haifa, Israel. [z]Institut für Physik, Universität Mainz, Mainz, Germany. [aa]CFNUL - Universidade de Lisboa, Faculdade de Ciências, Lisbon, Portugal.[bb]University of California at Irvine, Irvine, USA. [cc]University of Victoria, Victoria, Canada.

## 1. INTRODUCTION

ATLAS (A Toroidal LHC ApparatuS) is one of the four detectors currently being built around the LHC (Large Hadron Collider) at the European Organization for Nuclear Research (CERN) in Geneva, Switzerland. The LHC will collide protons at a center-of-mass energy of 14 TeV. ATLAS is a multipurpose detector designed to have a $4\pi$ hermeticity around the interaction region. The physics goals of ATLAS are numerous: Higgs and SUSY searches, Top, QCD, and B physics, as well as exotic searches. In addition, part of the excitement for reaching this energy frontier is the discovery potential associated with this unchartered territory. These physics requirements combined with a bunch crossing rate of 40 MHz in addition to an average of 25 inelastic proton-proton underlying interactions in each bunch crossing (at a design luminosity of $10^{34}\,cm^{-2}\,s^{-1}$) put very stringent constraints on the data acquisition and trigger system. The overall architecture of the three-level ATLAS trigger system is shown in Fig. 1. It is designed to reduce the nominal 40 MHz bunch crossing rate to a rate of about 200 Hz at which events, that will have a size of about 1.6 MB on average, will be written to mass storage. The first stage of the trigger, LVL1, is hardware-based and it reduces the rate to 75 kHz. Using the fast calorimeter and muon sub-detectors, it has a latency (time taken to form and distribute the LVL1 trigger decision) of 2.5 $\mu$s. During that time, the data from all the sub-detectors (about $10x$ electronic channels) are kept in pipeline memories. After the LVL1 decision, selected data fragments are transferred to the Readout Drivers (RODs) and then to the Readout Buffers (ROBs). The LVL1 result contains information about the type and thresholds of the accepted trigger (i.e Muon, Electromagnetic, Jets, etc..), and its geometrical position.

The second stage of the trigger system, LVL2, is software-based and it reduces the rate to about 2 kHz. With

the foreseen computing power for the LVL2 farm, we target an average execution time at LVL2 of 10 ms per event. In order to achieve this goal, the main characteristic of this stage is a fast rejection achieved by optimized trigger algorithms. The last stage of the trigger system, the Event Filter, occurs after the event building process. At this stage, the average execution time targeted is about 1s. The goal of the Event Filter is twofold: to reduce the rate to about 200 Hz, and to classify the events in different streams of interesting processes. Full calibration and alignment information is available at this stage. The Event Filter trigger algorithms have much in common with the offline algorithms and reuse of those is foreseen when possible. The LVL2 and the Event Filter stages are commonly referred to as the High Level Trigger (HLT).

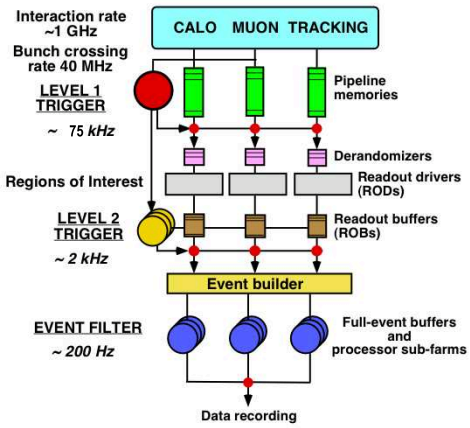


Figure 1: Block diagram of the Trigger/DAQ system.

The next section will describe briefly the main features of the HLT design [2].

## 2. HLT STRATEGY

### 2.1. The Region of Interest Mechanism

The Region of Interest (RoI) mechanism is used at LVL2 to significantly reduce the amount of data to be analyzed within its 10 ms target mean execution time, while retaining the full rejection power of a software selection, based on full granularity data from all the detectors.

All the information gathered at LVL1, like the geometrical position in $\eta$ and $\phi$ of the tagged objects and the thresholds they passed, is sent to the RoI Builder (RoIB) which combines it into a single record that is passed to Level2 Supervisors (L2SV). The position of the LVL1 RoI serves as a seed to request data around the region of the detector that contains the interesting signal; this way, only a small fraction of data will be asked to the online software and moved to the LVL2 Processing Units (L2PU), thus minimizing network bandwidth and processing time.
In particular, the conversion of a geometrical $(\eta, \phi)$ region into detector identifiers (unique number associated with an specific read-out channel), each corresponding to a sub-detector element, is performed by the HLT Region Selector [3], whose operation is depicted in Fig. 2; this tool uses information from the detector description to build fast lookup tables mapping each $(\eta, \phi)$ position into the sub-detector elements from which to request data.

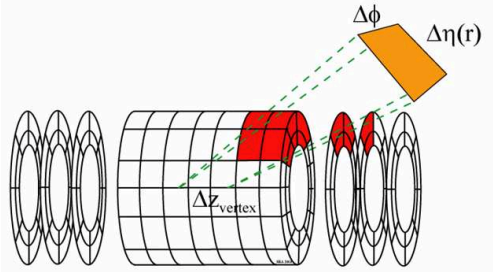


Figure 2: The Region Selector tool: each geometrical $(\eta, \phi)$ region is converted into a set of Detector Elements to be analyzed by LVL2 algorithms.

### 2.2. Algorithm Data Access

A fundamental part in the design of the HLT architecture is the way in which an HLT algorithm accesses the data. Fig. 3 shows a diagram with the main software components, and the flow of data between them. The idea behind the design is to ease the task of HLT algorithms, leaving the load of all the data handling operation to a data manager module. The HLT algorithm requests data in a RoI using the offline transient data store (Storegate [4]) as interface, and the Region of Interest package, a software component which returns Storegate pointers to the data inside the specified detector geometrical region. These data are in form of C++ objects, more suitable for the algorithm (e.g. vector of calorimeter cells which hold energy and position) than the data coming from the detector electronics which is in raw format (i.e. a binary data with the read-out channel information). The software which transforms one representation into another is the raw data converter. The raw data conversion is done on demand (the conversion into data objects is only done for the data inside the requested RoI), and it only occurs if the necessary objects are not already cached. This leads to a substantial reduction in the network and computation resources that would otherwise be required. It should be stressed that the same software is used in the offline and in the HLT online running environment. The only difference is that when executed offline the data source is a file while direct network access to ROSs is used in the LVL2, or to memory resident events in the EF case when running online.

### 2.3. Event Selection Software

The Event Selection Software (ESS) is one of the main components of the HLT system, and is the responsible for the classification and selection of the events. We saw in the previous subsection how the raw event data coming from

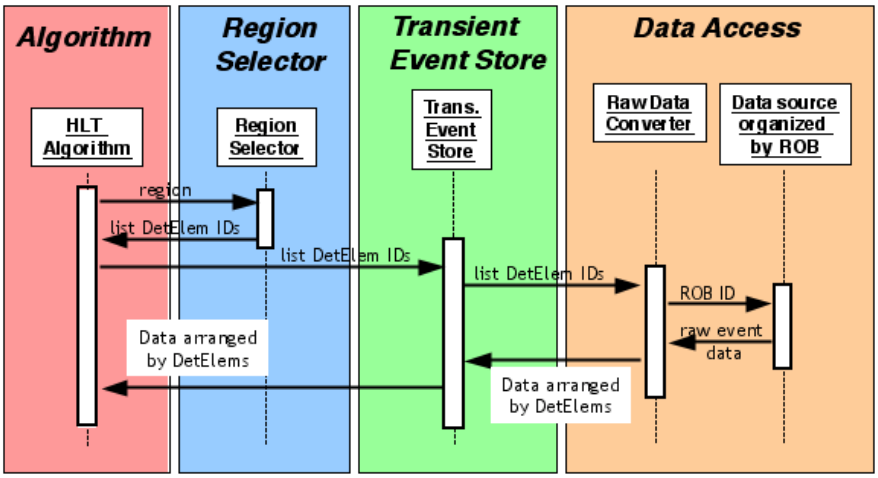


Figure 3: Algorithm data access.

the detectors, was converted on demand into C++ entities, and stored in memory for further processing. Abstract objects representing candidates such as electrons, muons, or $Z \rightarrow ee$ are reconstructed from these data by a set of HLT algorithms, and identified with the help of appropriate selection criteria. An event is selected if the reconstructed objects satisfy at least one of the physics signatures given in a trigger menu.

A key concept within the ESS infrastructure is the Steering mechanism[5]; motivated by the need to have fast and early rejection of uninteresting events in a flexible and configurable manner, and also to deal with special trigger configurations such as the pre-scale/force accept of some events. At the core of the ESS Steering is the Steering Controller[6], which is the software component in charge of the control, and proper guidance of HLT algorithms through the different steps leading to the validation of a final signature. It is designed in a way that allows full control of the algorithm execution within the HLT processing flow with changes in the configuration that do not need additional software compilation.

One of requirements is that the ESS must also be able to run directly in the offline software environment of ATLAS (ATHENA[7]). The benefits from this approach are multiple: this will facilitate the development of algorithms; this will allow the study of the boundary between LVL2 and Event Filter and it will lead to easy performance studies for physics analysis. The ESS needs therefore to comply with the control framework and services that are provided by the offline framework architecture. For this reason, ATHENA was adopted as the software framework running the ESS in both the EF, and (in a modified form due to design restrictions) the LVL2 processing units.

## 3. ELECTRON AND PHOTON SELECTION

Many interesting physical phenomena at LHC can lead to a final state containing isolated electrons and/or photons. They provide a clean signature, and are therefore important in the reconstruction of channels with a high statistical significance. Moreover, a common channel like $Z \rightarrow ee$ is a multipurpose tool with many key applications (i.e detector calibration, quick determination of electron identification efficiencies, etc..). The ESS running within the HLT must be therefore tuned in order to be as efficient as possible in its selection, while still rejecting most of the background (i.e. keeping the selected event rate within a certain imposed limit).

The procedure for the electron and photon selection[8][9] is as follows. At LVL2, the selection and further processing of potential candidates is guided by the previously described Region of Interest mechanism. LVL2 uses information on the energy and the direction of the electro-magnetic clusters selected by the LVL1 trigger and only the regions around these candidates are further analyzed. Thus, only part of the detector data needs to be processed, typically around 2% of the whole event in the case of the $e/\gamma$ triggers. The LVL2 selection for electrons and photons first analysis the shower shapes in the electromagnetic calorimeter and the leakage into the hadronic calorimeter. If a candidate is consistent with an electron it is further processed and in the next step tracks are searched for in the inner detector and the cluster and track quantities are compared. For photons tighter shower shape cuts are applied. In case the specified physics signatures are fulfilled the event is passed on to the EF. At this level the information of the complete event is available and either the LVL2 result can be used as a seed or the whole event can be reconstructed. Compared to LVL2 more precise calibrations and alignment are available. Similar to LVL2, electrons and photons are selected using the calorimeter

and the inner detector information. More time consuming algorithms such as bremsstrahlung recovery for electrons and conversion reconstruction for photons can be used.

Using realistic Monte-Carlo simulations of the expected behavior of the ATLAS detector, electronic noise and pile-up; the performance of the $e/\gamma$ triggers has been evaluated in terms of the efficiency for the signal channels, the rate expected for the selection, the data preparation times, and the algorithms execution times.

| **Trigger Step** | **Rate (Hz)** | **Efficiency (%)** |
|---|---|---|
| LVL2 Calo | $1948 \pm 46$ | $95.6 \pm 0.3$ |
| LVL2 Tracking | $364 \pm 21$ | $89.4 \pm 0.5$ |
| LVL2 Matching | $143 \pm 12$ | $87.7 \pm 0.6$ |
| EF Calo | $101 \pm 15$ | $86.1 \pm 0.6$ |
| EF Tracking | $71 \pm 10$ | $82.0 \pm 0.6$ |
| EF Matching | $34 \pm 6$ | $79.7 \pm 0.7$ |

Table 1: Performance of the single electron HLT trigger at low luminosity. The results are presented in a single sequence. Matching refers to position and energy-momentum matching between calorimeter clusters and reconstructed tracks (at LVL2 only precision tracks are used). The efficiencies are given for single electrons of pT = 25 GeV over the full rapidity range $|\eta| < 2.5$. The efficiencies and rates are given with respect to a LVL1 output efficiency of 95% and a LVL1 rate for e.m. clusters of 12 kHz. These numbers are still preliminary.

Table 1 shows the electron efficiencies and expected rates for the single electron trigger after each trigger step. This trigger is set up to select efficiently isolated electrons with a transverse energy ($E_T$) of at least 25 GeV (e25i) at start-up luminosity (L = $2 \times 10^{33}\ cm^{-2}s^{-1}$). For a electron efficiency of 80% with respect to LVL1 a rate of around 35 Hz has been found. The final rate comes mainly from real electrons (44% from b- and c-quark decays, 21% from converted photons, 19% from $W \rightarrow e\mu$ decays, 1% from $Z \rightarrow ee$ decays). Only 25% of the rate comes from fake clusters. If the rate for a trigger item from any level in the selection is too high, one can reduce it either by raising the $E_T$ threshold of the item or by tightening the selection criteria, which, however, result in a loss of efficiency in interesting physics events, partly recoverable by adding more exclusive triggers for the channels of interest. To ensure the physics programme at the LHC and the correct set-up of the trigger menus, cross-checks have been performed using important physics channels such as $H \rightarrow 4e$, $H \rightarrow \gamma\gamma$, $Z \rightarrow ee$, and $W \rightarrow e\mu$.

Table 2 shows the selection efficiencies for two samples of fully simulated Monte-Carlo $H \rightarrow 4e$, and $H \rightarrow \gamma\gamma$ events using realistic simulations of expected performance of the ATLAS detector, electronic noise and pile-up for both, start-up, and design luminosity (L = $1 \times 10^{34}\ cm^{-2}s^{-1}$). The efficiencies obtained for each trigger configuration (i.e. e25i represents a single isolated (i) electron (e), with $E_T$ greater than 25 GeV) demonstrate that the trigger menus for electrons and photons are well adapted for the physics programme envisaged at LHC (Higgs searches in this case)[10].

| **Trigger Item** | **Luminosity** | **Efficiency(%)** | |
|---|---|---|---|
| | $cm^{-2}s^{-1}$ | $H \rightarrow 4e$ | $H \rightarrow \gamma\gamma$ |
| e25i | $2 \times 10^{33}$ | $96.5 \pm 0.2$ | |
| 2e15i | $2 \times 10^{33}$ | $95.8 \pm 0.2$ | |
| e25 or 2e15i | $2 \times 10^{33}$ | $96.7 \pm 0.2$ | |
| e30i | $1 \times 10^{34}$ | $96.0 \pm 0.4$ | |
| 2e20i | $1 \times 10^{34}$ | $94.5 \pm 0.4$ | |
| e30 or 2e20i | $1 \times 10^{34}$ | $95.5 \pm 0.3$ | |
| $\gamma 60i$ | $2 \times 10^{33}$ | | $57.0 \pm 0.6$ |
| $2\gamma 20i$ | $2 \times 10^{33}$ | | $74.0 \pm 0.6$ |
| $\gamma 60i$ *or* $2\gamma 20i$ | $2 \times 10^{33}$ | | $83.0 \pm 0.5$ |

Table 2: Trigger Efficiencies(%) for the $H \rightarrow 4e$ ($100\,GeV < m_H < 150\,GeV$), and $H \rightarrow \gamma\gamma$ (120 GeV) channels at low, and design luminosity. The efficiency in this case is defined as the ratio of events passing a given trigger item (leftmost column ) with respect to an initial preselected sample ( minimum threshold requirement for the transverse energy ($E_T$), and within an $\eta$ range: $|\eta| < 1.52$, and $1.37 < |\eta| < 1.52$ outside barrel-endcap transition region for $H \rightarrow \gamma\gamma$ ).

In order to validate the chosen architecture, the selection of the electron and photon candidates has been integrated in test-beds and the whole system is being currently tested in the ATLAS combined test-beam. These tests are important in order to assess the system performance under real life conditions.

The algorithm execution times per RoI for calorimeter cluster reconstruction, and the corresponding data preparation time (raw data access time and the preprocessing time of these data in such a way, that they can be easily and efficiently used by the algorithms) were estimated for the LVL2 by means of a dedicated test-bed in a farm of 2.2GHz processors.

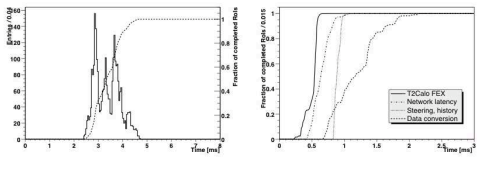


Figure 4: Total latency for RoI processing (shown at left) in the LVL2 calorimeter trigger for di-jet events at startup luminosity. The dotted curve is the integral of the distribution, showing that 95% of the events are processed within 5 ms. The four main contributions to the total latency are shown (right) as curves of integrals. The contributions are (in order of decreasing importance): data preparation and conversion, framework overheads, network access time, and algorithmic processing.

Fig. 4 shows the main contributions to the total latency

for a sample of di-jets events at start-up luminosity in a $\Delta\eta \times \Delta\phi = 0.3 \times 0.3$ RoIs. Pure algorithm execution is completed within $500\mu s$, while data access is typically completed within 1.8 ms for 95% of the events.

Continuous effort is put in improving these timings, nonetheless, they are already within target mean processing time at start-up ($\sim 10ms$).

## SUMMARY AND CONCLUSIONS

Given the LHC characteristics, the Trigger system have to face many challenges. The atlas collaboration have adopted a three-level trigger system, with the aim to bring down the initial interaction rate of $10^9$ Hz to to a rate of about 200 Hz at which events will be written to mass storage. This approach reduces substantially the cost in processing power & network bandwidth, but at the expenses of having a more complex design. The HLT architecture uses the RoI concept (this is a defining feature of ATLAS), along with a specialized data access scheme, and ESS, where only a few percentage of the data needs to be transfered and processed.

An effective selection of electrons and photons by the HLT ESS is of extreme importance, since they are involved as a final signature in many of the new physics phenomena expected to come out the LHC.

Using Monte-Carlo simulations the performance of the electron, and photon triggers has been evaluated in terms of the efficiency for the signal channels, the data preparation times, and the algorithms execution times. Preliminary results, look promising, and in agreement with physics, and technical design requirements.

In order to ensure the correct setup of the $e/\gamma$ trigger configuration, cross-checks have been performed using important physics channels such as $H \rightarrow 4e$, or $H \rightarrow \gamma\gamma$, showing that the trigger menus for electrons and photons are well adapted for the physics programme envisaged at LHC.

## ACKNOWLEDGMENTS

The authors wish to thank the HLT group for their support and assistance during the preparation of this work, in particular P. Conde Muíño, and V. Amaral for their last minute technical support.

## REFERENCES

[1] ATLAS TDAQ HLT group, http://atlas.web.cern.ch/Atlas/GROUPS/DAQTRIG/HLT/AUTHORLISTS/chep2004.pdf

[2] The Atlas Collaboration, *Atlas High Level Triggers, Data Acquisition and Controls, Technical Design Report*, CERN/LHCC/2003-022, 2003.

[3] S. Armstrong et al., "An Implementation of Region-of-Interest Selection for ATLAS High Level Trigger and Offline Software Environments", ATLAS Internal Note, ATL-DAQ-2003-014 (2003)

[4] P. Calafiura et al. TheStoreGate: a Data Model for the Atlas Software Architecture, Proceedings CHEP03, LaJolla, California, March24-28, 2003.

[5] G. Comune et al. The Algorithm Steering and Trigger Decision mechanism of the ATLAS High Level Trigger, Proceedings CHEP03, LaJolla, California, March24-28, 2003.

[6] M. Elsing et al., "Analysis and Conceptual Design of the HLT Selection Software", ATLAS Internal Note, ATL-DAQ-2002-013 (2002)

[7] Athena: User Guide and Tutorial, http://atlas.web.cern.ch/Atlas/GROUPS/SOFTWARE/OO/architecture/General/Tech.Doc/Manual/2.0.0-DRAFT/AthenaUserGuide.pdf

[8] S. González, T. Hansl-Kozanecka and M. Wielers, "Selection of $high - p_T$ electromagnetic clusters by the Second Level Trigger of ATLAS", ATLAS Internal Note, ATL-DAQ-2002-002 (2000)

[9] J.T.M Baines et al., "Performance Studies of the High Level Electron Trigger", ATLAS Internal Note, ATL-DAQ-2003-020 (2003)

[10] V. Perez Reale et al., "Triggering Standard Model Higgs processes in the ATLAS experiment", ATLAS Note, ATL-COM-PHYS-2004-051 (2004). Proceedings PHLHC 04, Vienna, Austria, 13 - 17 Jul 2004.